*Journal of Materials and Manufacturing 3(2): 32-40 (2024)*

Journal of Materials and Manufacturing

# Roughness and microstructure characterization of AISI 316L laser-powder bed fusion specimens after applying a vibration-assisted ball burnishing process

Eric Velázquez-Corral[a,*], Adrián Travieso-Disotuar[a,b], Ramón Jerez-Mesa[a], Montserrat Vilaseca[b], Clément Keller[c] and Gilles Dessein[c]

[a]*Mechanical Engineering Department, Universitat Politècnica de Catalunya, Av.Eduard Maristany 10-14, Barcelona, 08019, Spain*
(ORCID: 0000-0001-8037-7913), eric.velazquez.corral@upc.edu
(ORCID: 0009-0001-1254-7535), adrian.alberto.travieso@upc.edu
(ORCID: 0000-0002-5084-3108), ramon.jerez@upc.edu
[b]*Eurecat, Centre Tecnològic de Catalunya, Unit of Metallic and Ceramic Materials, Plaça de la Ciència, Barcelona, 08243, Spain*
(ORCID: 0000-0003-0472-0497), montserrat.vilaseca@eurecat.org
[c]*Laboratoire Génie de Production, Université de Technologie Tarbes Occitanie Pyrénées, 47 Avenue d'Azereix, Tarbes, 65000, France*
(ORCID: 0000-0002-2784-7450), clement.keller@uttop.fr
(ORCID: 0000-0003-3084-7985), gilles.dessein@uttop.fr

**Abstract**

The objective of this study is to analyze the effect of adding an ultrasonic vibration assistance within a ball burnishing (VABB) process onto cylindrical AISI 316L laser powder bed fusion (LPBF) specimens. The purpose of the specimens is to improve surface integrity, in terms of roughness reduction and microstructure reconstruction, to optimize the fatigue performance for testing samples according to ISO 1099:2017, reducing surface imperfections with burnishing. All printed specimens were manufactured in the Z direction using a laser power of 195W, a scanning speed of 900 mm/s, a hatch distance of 0.1 mm, a layer thickness of 40 µm, and a scan angle of 67°. The preliminary experimental campaign is based on a full factorial design of 3 variables (burnishing force, number of passes, and BB/VABB) with 2 levels for each. It was found that the estimated depth of affectation is 4-5 µm and 5-7 µm, for BB and VABB respectively, thus demonstrating the positive effect of the vibration assistance. The softening effect while deforming, caused by the vibration assistance, helped to reconstruct the surface, obtaining higher depths of affectation. In terms of topology, the surface average roughness for all specimens is within the range of 0.2-0.4 µm, showing an improvement of 74% in the best case compared to the machined surface. The material distribution parameters, Skewness and Kurtosis, show an almost perfect Gaussian distribution for all the specimens analyzed.

*Keywords:* Laser powder bed fusion; Ball burnishing; Surface integrity

## 1. Introduction

Additive manufacturing (AM), also known as 3D printing, represents a significant innovation in manufacturing processes. Unlike conventional subtractive methods such as machining and turning, that remove material to create a desired form, AM builds objects layer-by-layer from a digital design, saving thousands of kilograms of wasted material and production costs [1]. This technology offers significant advantages, among them it can highlight the ability to produce complex geometries, lightweight structures, and parts with integrated functionalities that are impossible to achieve with conventional techniques [2]. AM has seen rapid advancements

* Corresponding author
*E-mail addresses:eric.velazquez.corral@upc.edu*
DOI: 10.5281/zenodo.14274784
Received: 23 August 2024, Revised: 29 October 2024, Accepted: 26 November 2024
ISSN: 2822-6054 

in recent years, with a growing variety of technologies and materials being explored for diverse applications across various industries.

While metal AM offers a promising future, this process faces several challenges that limit its widespread adoption. Achieving optimal surface integrity for the finished components is a major challenge [3]. Unlike traditional manufacturing methods that can achieve smooth surfaces, the layer-by-layer nature of AM inherently creates a stair-step effect on the surface. This can lead to increased roughness, presence of unfused particles, and potential weaknesses that may compromise fatigue strength, wear resistance, and overall performance of the part [4]. Ensuring consistent quality and repeatability across builds remains an ongoing area of development for metal AM, since the wide range of parameters introduces several variables, which influences the outcome of the process, triggering the defects [5]. Recent investigations are focused towards exploring different process parameters, like laser power and scan strategy, to minimize these effects [6]. Additionally, several post-processing techniques [7,8] are being actively researched to improve the surface finish and address residual stresses within the material. Understanding and optimizing surface integrity remains a crucial area of focus for ensuring the functionality and reliability of metal additive manufactured (AMed) components.

Among a wide list of post-processes techniques, this study is focused on the interaction of ball burnishing technology with the surface quality and mechanical properties of AMed parts. This process is based on the concept of elastoplastic deformation of materials by applying a force either perpendicular or angular to the plane of the surface by means of a ball-end tool [9]. As the ball passes over the surface, the material deforms and flattens, leaving the surface more compact and smoother than that obtained from the manufacturing process. Besides, the force applied is a considerable variable since as it changes, the hardness, residual stress, and microstructure change [10]. Ball burnishing is integrated into a vibrational assisted system (VABB) for increasing the performance of the process on the surface. This variation allows control of the force and the compression action which makes it possible to decrease the quasi-static stress necessary to deform a material [11,12].

Achieving high-quality surfaces is crucial for AMed components, and the VABB process needs to adapt to meet this challenge. Research by Sanguedolce et al. [13] highlights the promise of burnishing, demonstrating improvements in surface roughness, hardness, and residual stresses. Their findings suggest burnishing can be effectively integrated into industrial AM workflows, offering customization and new opportunities. Moreover, Karthick Raaj et al. [14] study on grinding and burnishing of AMed alloy 718 samples confirms these benefits, achieving the lowest microporosity and surface roughness. Similar results were obtained by Yaman et al. [15] who focused on enhancing the surface integrity of AMed Inconel 718 through roller burnishing. Their work identified burnishing force and speed as critical parameters for optimizing the process. These studies collectively demonstrate the effectiveness of burnishing techniques in improving the surface integrity of AMed components.

The integration of ball burnishing into a vibrational assisted system enhances the process performance by allowing control over the applied force and compression action to reduce the quasi-static stress needed for material deformation. This underscores the potential of burnishing to be effectively integrated into industrial AM workflows for enhancing the customization and the quality of metal AMed. With this in mind, the objective of the article is to provide an analysis of the effect of VABB on laser powder bed fusion (LPBF) printed AISI 316L metal surfaces.

The novelty of this investigation is the analysis of the vibration assisted ball burnishing process with a lathe burnishing tool on LPBF AISI 316L. It has been previously analysed on traditional laminated material, but not on LPBF materials for this specific application. Besides, there is an interest to show which parameters can improve the performance of the process and how they relate to each other by analyzing not only the surface roughness, but also by analyzing microstructural subsurface effects.

## 2. Material and Methods

### *2.1. Fabrication and specifications*

The particle size of the AISI 316L stainless steel was within the range of 15-45 μm. The powder used in this study was a mixture of 10% fresh powder and 90% powder that was recovered from prior processing and sieved

before reuse. The chemical composition specified by the manufacturer is listed in Table 1. Specimens were processed using a ProX300B printer.

**Table 1.** Chemical composition of AISI 316L LPBF by element in wt. (%)

| Material | Chemical composition by element in wt. (%) | | | | | | | | |
|---|---|---|---|---|---|---|---|---|---|
| AISI 316L LPBF | C | Fe | Cr | Ni | Mo | Mn | Si | P | S |
| | <0.03 | Bal. | 16-18 | 10-13 | 2-2.5 | <2.00 | <1.00 | <0.04 | <0.03 |

Target specimens are designed according to the ISO 1099:2017 standard for uniaxial fatigue testing, so Ø16-mm bars will be printed in the Z-axis direction. The printing parameters selected were based on a previous pilot experience, where it was tried to reduce the average roughness of the specimens, and kept constant for all the specimens manufactured. Laser Power P was set to 195W, scanning speed v_s was 900 mm/s, hatch distance HD was 0.1 mm, layer thickness LT was 40 μm and the scan angle φ was set to 67°.

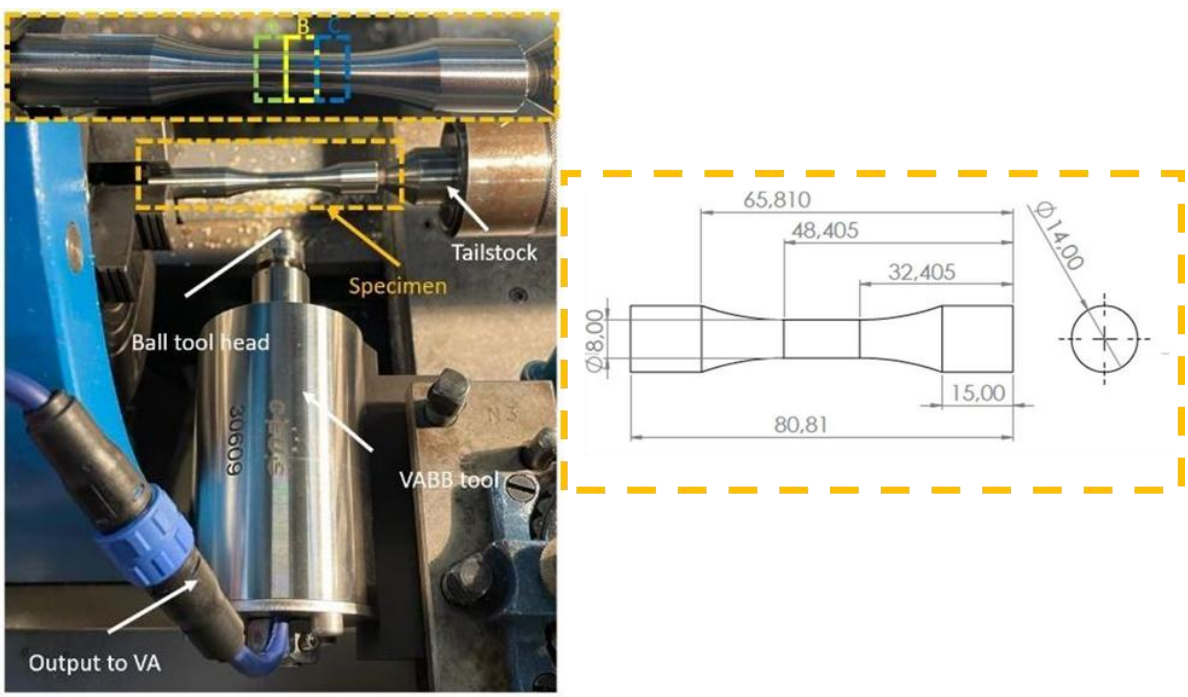


Fig. 1. Ball burnishing setup for the specimen's fabrication and dimensions.

After printing, all specimens were machined in a 3-axis Cazenueve Optica 360 turning machine with a DCMT11T308 insert, using a cutting speed of 65 m/min and a feed of 0.07 mm/rev for the finishing. Once the machining is finished and it is ensured that accomplishes all dimensional requirements after turning, the ball burnishing process is applied, alternating between VABB and BB operation over the surface of interest on the workpiece. The tool used is based on a calibrated spring in order to calibrate the burnishing force applied. Also contains a piezoelectric-sonotrode module that gets excited at a frequency of 40 kHz, having a maximum amplitude of oscillation of 8μm at the ball top. The balls used for this experiment are made of tungsten carbide balls, seven 2-mm diameter balls and one 10-mm diameter are used for the final setup. In fact, the bigger ball is responsible for deforming the peaks of the surface by rolling, while the small ones allow totally free rotation

and lodging inside the tool cap of the bigger ball. For material saving, 3 burnishing patches of 5 mm length were done, so considering also a non-treated and only turned patch, the final specimen distribution is the one specified in Table 2:

**Table 2** Parameters of the burnishing process

| **Factor** | **Symbol** | **Level** | |
|---|---|---|---|
| | | 1 | 2 |
| Burnishing Force (N) | *Fb* | 160 | 240 |
| Number of passes | *np* | 1 | 3 |
| Burnishing process | *Pr.* | BB | VABB |

| **Factor** | *Fb* (N) | *np* | *Pr.* | **Nomenclature** |
|---|---|---|---|---|
| Raw | - | - | - | R |
| Machined | - | - | - | M |
| 1A | 160 | 1 | BB | 160-1-BB |
| 1B | 160 | 3 | BB | 160-3-BB |
| 1C | 160 | 1 | VABB | 160-1-VABB |
| 2A | 160 | 3 | VABB | 160-3-VABB |
| 2B | 240 | 1 | BB | 240-1-BB |
| 2C | 240 | 3 | BB | 240-3-BB |
| 3A | 240 | 1 | VABB | 240-1-VABB |
| 3B | 240 | 3 | VABB | 240-3-VABB |

### *2.2. Topography analysis*

The topographical parameters analyzed, for the prior surface, in this investigation are the amplitude parameters specified in the standard ISO 25178, namely Sa (represents the arithmetical deviation of the roughness profile of the sampling length), Sz (the sum of the largest peak height value and the largest pit depth value), and Ssk and Sku (distribution of the material at different heights on the surface). To analyze the textures, a non-contact ALICONA Infinite Focus G5 3D profilometer (Alicona Imaging GmbH, Raaba, Austria) is used, acquiring 4 x 2 mm patches with a 1 μm sampling interval. The acquired datasets were processed using Mountains 9.2 software to generate S-L surfaces. This involved applying an F filter to eliminate the surface form from the original height data, an S filter to remove acquisition noise, and an L filter to eliminate surface waviness. According to ISO 25178-3, the cutoff values for the S filter and L filter were 5.00 μm and 0.8 mm, respectively for burnishing and machined samples, and 8.00 μm and 0.8 mm for the raw specimen. Additionally, remove cylinder form operator was applied.

### *2.3. Scanning Electron Microscopy (SEM)*

The analysis of the microstructure is done on a sectional cut surface of both burnished treated samples, after mirror polishing and chemically etching the surfaces with oxalic acid during 70 seconds at a 3.5 V of current-voltage to reveal the microstructure. To see this effect, a JEOL JSM-7001F scanning electron microscopy (SEM) was used.

## 3. Results and Discussion

### *3.1. Roughness analysis*

The original roughness for all specimens after turning was fixed to an initial average of $0.8 \pm 0.1$ , and the burnishing conditions applied are shown in Table 3.

**Table 3** Topography results for all AISI 316L LPBF specimens

| **Sample** | *Sa (μm)* | *ΔSa (%)* | *Sz (μm)* | *Ssk* | *Sku* |
|---|---|---|---|---|---|
| R | 15.35 | - | 115.8 | -0.1344 | 2.913 |
| M | 0.8293 | ref. | 7.666 | 0.1167 | 2.790 |
| 160-1-BB | 0.2379 | 71 | 2.773 | 0.0599 | 3.305 |
| 160-3-BB | 0.2338 | 72 | 3.074 | 0.2458 | 3.653 |
| 160-1-VABB | 0.2346 | 72 | 2.958 | 0.0186 | 3.733 |
| 160-3-VABB | 0.2189 | 74 | 2.710 | -0.2120 | 3.533 |
| 240-1-BB | 0.2974 | 64 | 4.360 | 0.2365 | 3.801 |
| 240-3-BB | 0.3833 | 54 | 4.064 | -0.1232 | 3.023 |
| 240-1-VABB | 0.4079 | 51 | 3.767 | -0.0026 | 3.015 |
| 240-3-VABB | 0.3834 | 54 | 4.673 | -0.1769 | 3.384 |

In all burnished specimens analyzed, the average roughness Sa and the maximum profile height difference Sz were improved from the machined specimen on LPBF specimens (see Fig.2), as it was expected [16, 17]. However, it can be seen that applying a lower level of force (160 N) is more beneficial than the higher level tested. This may be due to the excess of plastic deformation exerted, eventually producing flaking and deterioration of the texture. The increase of the work-hardening effect on the surface is provoked by repeated plastic deformation, being an excess of force or several passes applied [18]. In terms of increasing the number of passes, the general trend is to slightly decrease the average roughness. This can be explained by the fact that the ball is rolling and smoothing out the bulged edges of the initial machining or the previous pass, so the probability of deforming the asperities is increased, until a determined plastic deformation point where the texture may start deteriorating. Concerning the vibration assistance, a small positive effect is detected if specimens with same force and number of passes are compared, this is explained by the addition of the kinematic energy of the vibration assistance, thus enhancing the work-hardening during the deformation process. The best results are obtained for the specimen 160-3-VABB, obtaining an average roughness reduction of 74% compared to the machined surface.

In terms of Skewness and Kurtosis, results determine that all surfaces measured present an almost perfect material distribution, considered Gaussian when Ssk is equal to 0 and Sku is equal to 3. One remark noticed is that burnishing, assisted or not, tends to obtain leptokurtic surfaces while the raw and machined surfaces were originally platykurtic. This tendency agrees with the 316L's burnishing bibliography [19, 20].

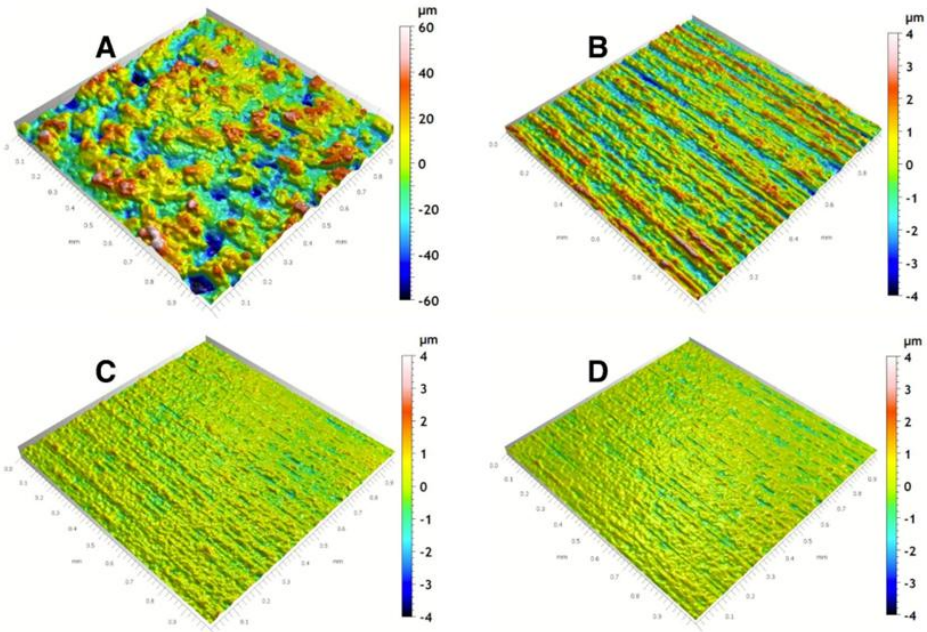


**Fig. 2.** Figures of textures acquired for different processes: (a) Raw. (b) Machined (c) Ball- burnished. (d) Vibration-assisted ball-burnished

### *3.2. Microstructure analysis*

The micrographs depicted in Fig.3 illustrate cross-sectional views of samples 240-3-BB subjected to ball burnishing (BB) and 240-3-VABB subjected to vibration-assisted ball burnishing (VABB). Additionally, a section of a non-burnished sample was extracted to facilitate a comparison of the resulting microstructures. The overall picture provides a view of austenite grains, defining the fundamental microstructure observed in these AISI 316L LPBF specimens.

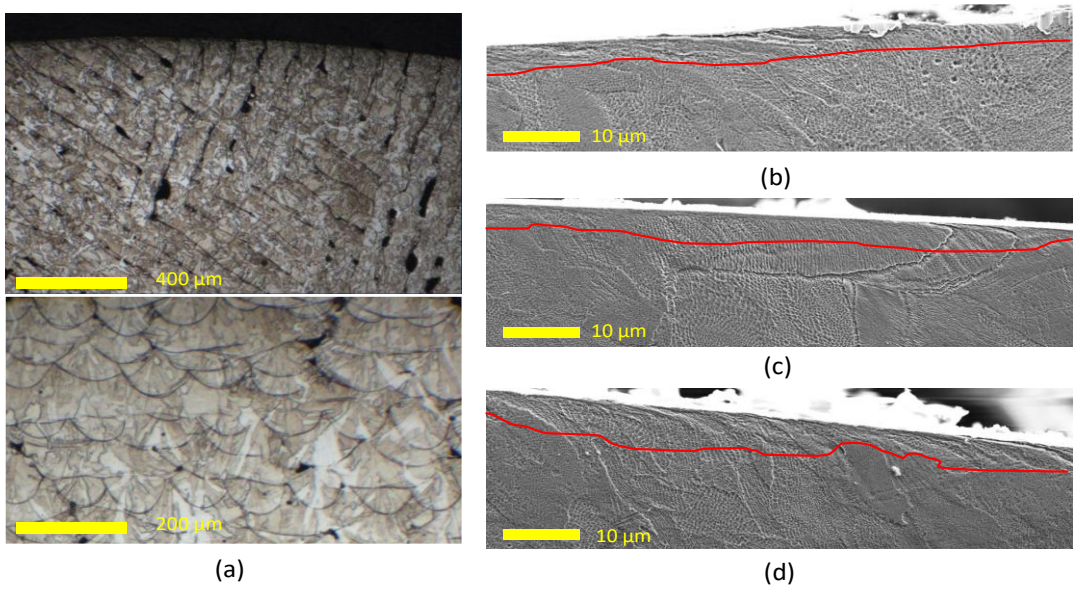


**Fig. 3.** Microstructure of specimens: (a) Bulk material; (b) M; (c) 240-3-BB; (d) 240-3-VABB.

The 316L LPBF bulk material is mainly composed of austenite grains with ferrite phase inhibited during the printing process, having several large elongated grains at meltpool or several meltpools scale in the building direction (see Fig.3 (a)). This material has a grain structure very different from the wrought 316L. At a finer scale a cellular structure is observed resulting from microsegregation dislocation stacking.

All specimens show plastic deformation boundaries at the surface. A new reorientation of the grains, in the direction of the turning and/or burnishing, is presented. Firstly, the specimen M affectation in depth is estimated between 3 to 5 µm due to the shearing induced by the cutting forces exerted during the turning process (see Fig. 3 (b)). Secondly, the 240-3-BB specimen presents a major density of plastic deformation, in terms of depth of affectation and also by the deformation mechanism. In this case, the depth is estimated at 4-5 µm and also presents deformation bands compatible with twinning formations at some zones of the subsurface (see Fig. 3 (c)). This effect could lead to an increase of the superficial hardness and compressive residual stresses due to a possible grain refinement [21]. Thirdly, the 240-3-VABB specimen presents a slight increase in depth affectation compared to the rest of the specimen, estimated at 5-7 µm (see Fig. 3 (d)). This is caused by the increment of pressure due to the superimposition of dynamic and static forces and the acoustoplastic phenomena. Then the positive effect of the vibration assistance is demonstrated in this material and under the conditions tested.

## 4. Conclusion

With all the tests and analyses performed, it can be concluded that:

- Ball burnishing improves the average roughness of AISI 316L shaft surfaces, and the vibration assistance slightly improves the texture when it is compared to traditional ball burnishing. The best parameters found in this study correspond to 160 N of force, three passes, and the activation of the vibration assistance. However, if an excessive force is applied, the effect of the vibration assistance is reduced and can also be detrimental to the topology enhancement.
- The VABB process provokes a larger plastic deformation onto AISI 316L LPBF cylindrical surfaces, which may converge in a hardening effect at more depth from the surface, than BB. This effect may also enhance the compressive residual stress, which also may converge in larger fatigue strength in future tests.

These results confirm the positive effect of vibration-assisted ball burnishing compared to conventional ball burnishing in terms of roughness reduction and increase of the depth of affectation in the subsurface. However, further topics should be analyzed. Firstly, the microstructure observations point to a possible hardening and increase of the residual stresses at the surface and eventually improve the fatigue strength, but the search of the optimal printing and burnishing parameters should be done. Also, it would be necessary to perform an EBSD and TEM analysis at the surface to better understand the localized plastic deformation induced at the coating, while characterizing the deformed crystals' reorientation and grain refinement.

**References**

[1] Pérez, M., Carou, D., Rubio, E. M., & Teti, R. (2020). Current advances in additive manufacturing. Procedia CIRP, 88, 439–444.
[2] Sun, C., Wang, Y., McMurtrey, M. D., Jerred, N. D., Liou, F., & Li, J. (2021). Additive manufacturing for energy: A review. Applied Energy, 282, 116041.
[3] Santos, V., Uddin, M., & Hall, C. (2023). Mechanical Surface Treatments for Controlling Surface Integrity and Corrosion Resistance of Mg Alloy Implants: A Review. Journal of Functional Biomaterials, 14(5), 242.
[4] Haghdadi, N., Laleh, M., Moyle, M., & Primig, S. (2021). Additive manufacturing of steels: a review of achievements and challenges. Journal of Materials Science, 56(1), 64–107.
[5] Mojumder, S., Gan, Z., Li, Y., Amin, A. A., & Liu, W. K. (2023). Linking process parameters with lack-of-fusion porosity for laser powder bed fusion metal additive manufacturing. Additive Manufacturing, 68, 103500.
[6] Gockel, J., Sheridan, L., Koerper, B., & Whip, B. (2019). The influence of additive manufacturing processing parameters on surface roughness and fatigue life. International Journal of Fatigue, 124, 380–388.
[7] Mahmood, M. A., Chioibasu, D., Ur Rehman, A., Mihai, S., & Popescu, A. C. (2022). Post-Processing Techniques to Enhance the Quality of Metallic Parts Produced by Additive Manufacturing. Metals, 12(1), 77.
[8] Peng, X., Kong, L., Fuh, J. Y. H., & Wang, H. (2021). A Review of Post-Processing Technologies in Additive Manufacturing. Journal of Manufacturing and Materials Processing, 5(2), 38.
[9] Velázquez-Corral, E., Wagner, V., Jerez-Mesa, R., Lluma, J., Travieso-Rodriguez, J. A., & Dessein, G. (2023). Analysis of Ultrasonic Vibration-Assisted Ball Burnishing Process on the Tribological Behavior of AISI 316L Cylindrical Specimens. Materials, 16(16), 5595.
[10] Gomez-Gras, G., Travieso-Rodríguez, J. A., González-Rojas, H. A., Nápoles-Alberro, A., Carrillo, F. J., & Dessein, G. (2015). Study of a ball-burnishing vibration-assisted process. Proceedings of the Institution of Mechanical Engineers, Part B: Journal of Engineering Manufacture, 229(1), 172-177.
[11] F. Blaha and B. Langenecker, “Elongation of zinc monocrystals under ultrasonic action,” Die Naturwiss, vol. 42, p. 556, 1955.
[12] Jerez-Mesa, R., Travieso-Rodriguez, J. A., Gomez-Gras, G., & Lluma-Fuentes, J. (2018). Development, characterization and test of an ultrasonic vibration-assisted ball burnishing tool. Journal of Materials Processing Technology, 257, 203-212.
[13] Sanguedolce, M., Rotella, G., Saffioti, M. R., & Filice, L. (2022). Burnishing of AM materials to obtain high performance part surfaces. Journal of Industrial Engineering and Management (JIEM), 15(1), 92-102.
[14] Raaj, R. K., Anirudh, P. V., Karunakaran, C., Kannan, C., Jahagirdar, A., Joshi, S., & Balan, A. S. S. (2020). Exploring grinding and burnishing as surface post-treatment options for electron beam additive manufactured Alloy 718. Surface and Coatings Technology, 397, 126063. doi:
[15] Yaman, N., Sunay, N., Kaya, M., & Kaynak, Y. (2022). Enhancing surface integrity of additively manufactured Inconel 718 by roller burnishing process. Procedia CIRP, 108, 681-686.

[16] Teimouri, R., Sohrabpoor, H., Grabowski, M., Wyszyński, D., Skoczypiec, S., & Raghavendra, R. (2022). Simulation of surface roughness evolution of additively manufactured material fabricated by laser powder bed fusion and post-processed by burnishing. Journal of Manufacturing Processes, 84, 10-27.
[17] Varga, G., Dezső, G., & Szigeti, F. (2022). Surface roughness improvement by sliding friction burnishing of parts produced by selective laser melting of Ti6Al4V titanium alloy. Machines, 10(5), 400.
[18] El-Taweel, T. A., & El-Axir, M. H. (2009). Analysis and optimization of the ball burnishing process through the Taguchi technique. The International Journal of Advanced Manufacturing Technology, 41, 301-310.
[19] Amanov, A., Lee, S. W., & Pyun, Y. S. (2017). Low friction and high strength of 316L stainless steel tubing for biomedical applications. Materials Science and Engineering: C, 71, 176-185.
[20] Attabi, S., Himour, A., Laouar, L., & Motallebzadeh, A. (2022). Surface Integrity of Ball Burnished 316L Stainless Steel. In Stainless Steels. IntechOpen.
[21] Agrawal, A. K., & Singh, A. (2017). Limitations on the hardness increase in 316L stainless steel under dynamic plastic deformation. Materials Science and Engineering: A, 687, 306-312.